Kovove Mater. 62 2024 253–266
DOI: 10.31577/km.2024.4.253

Study on the microstructure and mechanical properties of annealed TC4/6061/AZ31B/6061/TC4 symmetrical clad sheets

Xia Yang[1]*, Huitong Cui[1], Cunlong Zhou[1], Rui Zheng[2], Zhuojie Li[1]

[1] *College of Mechanical Engineering, Taiyuan University of Science and Technology, Taiyuan 030024, P. R. China*
[2] *CRRC DATONG CO., LTD., Datong 037006, P. R. China*

Received 3 April 2024, received in revised form 18 September 2024, accepted 2 October 2024

Abstract

In this study, five-layer symmetric clad sheets of TC4/6061/AZ31B/6061/TC4 were successfully prepared by hot rolling, and then the clad sheets were subjected to annealing treatments with different annealing conditions. The effects of annealing treatments on the mechanical properties and microstructure were explored. The results showed that the recovery and recrystallization process of magnesium alloy were fully strengthened, and the thickness of the elemental diffusion layer at the Ti/Al and Al/Mg combined interface increased with the increase in annealing temperature and holding time. When the annealing temperature exceeded 300 ℃, the Al/Mg combined interface generated two intermediate compounds, Al_3Mg_2 and $Mg_{17}Al_{12}$. Due to the existence of intermediate compounds, the mechanical properties of the clad sheets were greatly reduced, but the hardness value of the Al/Mg interface was higher than that of the center of the aluminum and magnesium layers. When the annealing temperature is 200 ℃ for 2 h, the tensile strength and the elongation of the clad sheets reach the maximum, and the magnesium layer has the most uniform grain organization at the same time.

K e y w o r d s: Ti/Al/Mg/Al/Ti clad sheets, hot rolling, microstructure, annealing, mechanical property

1. Introduction

With the rapid development of the machinery manufacturing industry, traditional single metal can no longer meet the needs of advanced manufacturing, so multi-metal layered composites have emerged [1–3]. At present, the preparation methods of clad sheets mainly include the explosive composite method [4–6], a rolling composite method [7–9], the extrusion composite method [10, 11], and the forging composite method [12, 13]. The rolling composite method is widely used because of the advantages of high efficiency and low cost. Magnesium alloy is widely used in industry, but its low plasticity and poor corrosion resistance restrict its further development [14, 15]. Therefore, many scholars began to explore a solution to cover the surface of a magnesium alloy with a metal layer with good corrosion resistance.

Because aluminum alloy has the characteristics of strong corrosion resistance, light weight and good plasticity, rolling composite of aluminum alloy and magnesium alloy can not only enhance the corrosion resistance of the plate, but also improve the overall formability of the plate. However, the internal dislocation density of each layer is large due to the processing-hardening effect. Therefore, the clad sheets prepared by hot rolling have a high residual stress. The reasonable annealing process benefits the dynamic recrystallization of the metal plate to eliminate the residual stress inside the clad sheets. Z. Q. Chen et al. found that the thickness of the diffusion layer at the interface of the explosive Mg/Al clad sheets increased with annealing temperature and holding time, and the tensile strength and elongation of the clad sheets reached in these aspects maximum at 200 ℃ for 2 h [16]. H. H. Nie found when the annealing temperature exceeded 300 ℃, two metal compounds $Mg_{17}Al_{12}$ and Al_3Mg_2 were generated at the Mg/Al interface [17].

*Corresponding author: tel.:+86-15035122963; e-mail address: xiay06@163.com

Table 1. Chemical composition of 6061 and AZ31B (wt.%)

Element	Si	Fe	Cu	Mn	Cr	Zn	Ca	Al	Mg
AZ31B	0.07	–	0.01	0.70	–	1.4	0.04	3.2	Bal.
6061	0.61	0.40	0.24	0.14	0.10	0.05	–	Bal.	1.03

Table 2. Element composition of TC4 (wt.%)

Element	Al	V	Fe	C	N	H	O	Ti
TC4	6.8	4.5	0.30	0.10	0.05	0.015	0.20	Bal.

Table 3. Rolling process parameters

Roll diameter (mm)	Rolling speed ($m\,s^{-1}$)	Rolling temperature (℃)	Relative reduction (%)
320	0.1	450	33

X. P. Zhang found that the grain size and diffusion layer thickness of Al/Mg/Al alloy laminated composites prepared by hot rolling highly depended on the reduction rate and rolling temperature [18]. J. J. Zhang analyzed the elastic constants and mechanical properties of the metal compound layer at the interface of the Al/Mg/Al laminated plate after annealing [19]. P. J. Wang studied the microstructure evolution at the interface during the annealing of Mg/Al clad sheets [20]. A. X. Zhang et al. studied a method of using hard-plate bonding to improve the defect of excessive stress in the process of accumulative roll-bonding (ARB) [21]. However, in harsh environments such as aerospace, marine, and chemical industry fields, the requirements for material properties are very high, especially in the corrosion resistance, strength, stiffness, and other aspects, and Mg/Al clad sheets have great disadvantages compared with other materials in these aspects. Titanium alloy has the advantages of high strength, good corrosion resistance, and so on. Therefore, the titanium alloy layer is added to the Mg/Al clad sheets to obtain the Ti/Mg/Al clad sheets, which can improve the overall specific stiffness and specific strength of Mg/Al clad sheets and increase the service life of the sheets. Y. J. Mi investigated the microstructure and mechanical properties in different directions of the Ti/Al/Mg/Al/Ti clad sheets prepared by hot rolling and explored the anisotropic behavior of the rolled state [22]. T. L. Wang investigated the microstructure evolution of the combined interface of Ti/Al/Mg clad sheets [23]. P. J. Wang discussed the effect of rolling reduction on the microstructure evolution and mechanical properties of Ti/Mg/Al clad sheets [24]. H. H. Nei et al. focused on the crack initiation of intermetallic compounds and diffusion layers in Ti/Mg/Al clad sheets [25].

In this paper, with TC4 titanium alloy plate, 6061 aluminum alloy plate, and AZ31B magnesium alloy plate as raw materials, Ti/Al/Mg/Al/Ti five layers symmetrical clad sheets were prepared by hot rolling and annealed to eliminate the residual stress inside the clad sheets. In order to effectively improve the comprehensive performance of the clad sheets, the influence of the annealing process on the microtissue performance and mechanical properties of the clad sheets was studied, and the optimal annealing process of Ti/Al/Mg/Al/Ti clad sheets was determined.

2. Experimental materials and methods

2.1. Rolling and annealing experiments

Magnesium alloy AZ31B was selected as the base layer, with a size of 150 mm × 80 mm × 2 mm; aluminum alloy 6061 was selected as the transition layer, with size of 150 mm × 80 mm × 1 mm; titanium alloy was selected as the cover layer, with size of 150 mm × 80 mm × 0.5 mm. The chemical compositions are shown in Tables 1, 2.

The surface of each plate was fully polished and cleaned with anhydrous ethanol, and the billets were prepared in the order of Ti/Al/Mg/Al/Ti. To prevent sliding between the plates during hot rolling, the plates were riveted by using rivets. The fixed plates were heated to 450℃ in a box-type resistance furnace, held for 12 min, and then taken out rapidly for hot rolling; the rolling process parameters are shown in Table 3. After rolling, the clad sheets prepared by rolling were annealed according to the annealing process parameters shown in Table 4 and cooled in air. The preparation process for the Ti/Al/Mg/Al/Ti clad sheets and the experimental sample fabrication process are shown in Fig. 1.

Table 4. Annealing process parameters

No. of clad sheet	Annealing temperature (℃)	Holding time (h)
1	–	–
2	200	0.5
3	200	1
4	200	2
5	300	2
6	400	2

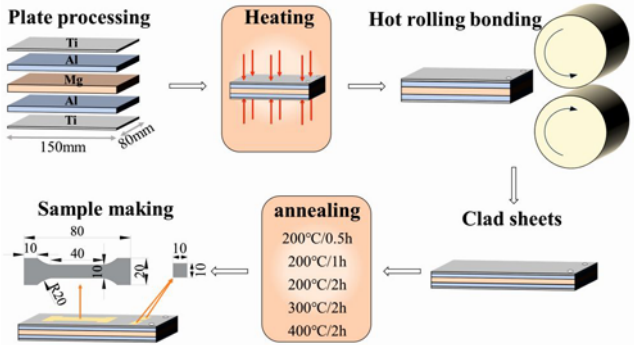

Fig. 1. The Ti/Al/Mg/Al/Ti clad sheets preparation process.

2.2. Microscopic characterization and mechanical properties test

To perform microscopic characterization and test mechanical properties of the Ti/Al/Mg/Al/Ti clad sheets, according to relevant standards, the clad sheets were cut by using an EDM wire-cutter to produce the metallographic samples, tensile samples, and hardness test samples, as shown in Fig. 1.

The tensile samples were subjected to tensile tests on a WDW-200E universal testing machine at the tensile speed of 0.5 mm min^{-1}. The yield strength (YS), ultimate tensile strength (UTS), and elongation (EL) were obtained from the stress-engineering strain curve.

The microscopic samples were mechanically polished using sandpaper and diamond polishing paste until they resembled a mirror surface. The microstructure of the Mg layer was observed by etching with picric acid. The interface morphology of the metallographic samples and fracture of the tensile samples were observed by Zeiss Auriga field emission electron microscope. The energy dispersive spectrometer (EDS) was used to scan the bonding interface of each layer of the metallographic sample and confirm the elemental composition of the Mg/Al bonding interface.

To observe the hardness change of the Ti layer, Al layer, Mg layer, and the interface of each layer in the Ti/Al/Mg/Al/Ti clad sheet under different annealing processes, the hardness test sample was measured by FM-ARS9000 Vickers hardness tester, with a measured load of 50 g and a loading time of 10 s.

3. Experimental results and discussion

3.1. Microstructure of Mg layer

Figure 2a shows the metallographic microstructure of the Mg layer of the clad sheet in a rolled state. Figures 2b–d show the change in the metallographic organization of the Mg layer with the annealing time at 200 ℃. Figures 2d–f show the metallographic organization of the Mg layer under different annealing temperatures when the annealing time was 2 h. As can be seen from Fig. 2a, the Mg layer in the rolled state mainly contained two kinds of grains with obvious differences in size: one was the coarse grains produced in the hot rolling process, and the other was the fine dynamic recrystallization (DRX) grains produced in the hot rolling process. From Figs. 2a–d, the recovery and recrystallization processes were sufficiently strengthened with the extension of the annealing time. The recrystallized grains continued to generate and grow, and the dynamically recrystallized grains generated during hot rolling also began to grow. Figure 2d shows the Mg layer metallographic microstructure at 200 ℃ for 2 h; it can be seen the grains of the Mg layer metallographic microstructure were basically isoaxial, and the grain size gradually tended to uniform. At this time, the Mg layer metallographic microstructure had reached the degree of complete recrystallization, and the stored energy produced by plastic deformation had been released. After completing the recrystallization process, when the temperature continued to rise, it entered the grain growth stage, as shown in Figs. 2e,f. With the increase in annealing temperature, the Mg layer grains gradually increased. When the annealing temperature reached 400 ℃, the fine grains almost disappeared, and there were only uniform large grains.

3.2. Interface morphology and elemental diffusion analysis

Figure 3 illustrates the interface morphology and element diffusion distribution of Ti/Al/Mg/Al/Ti clad sheets under different annealing conditions. As

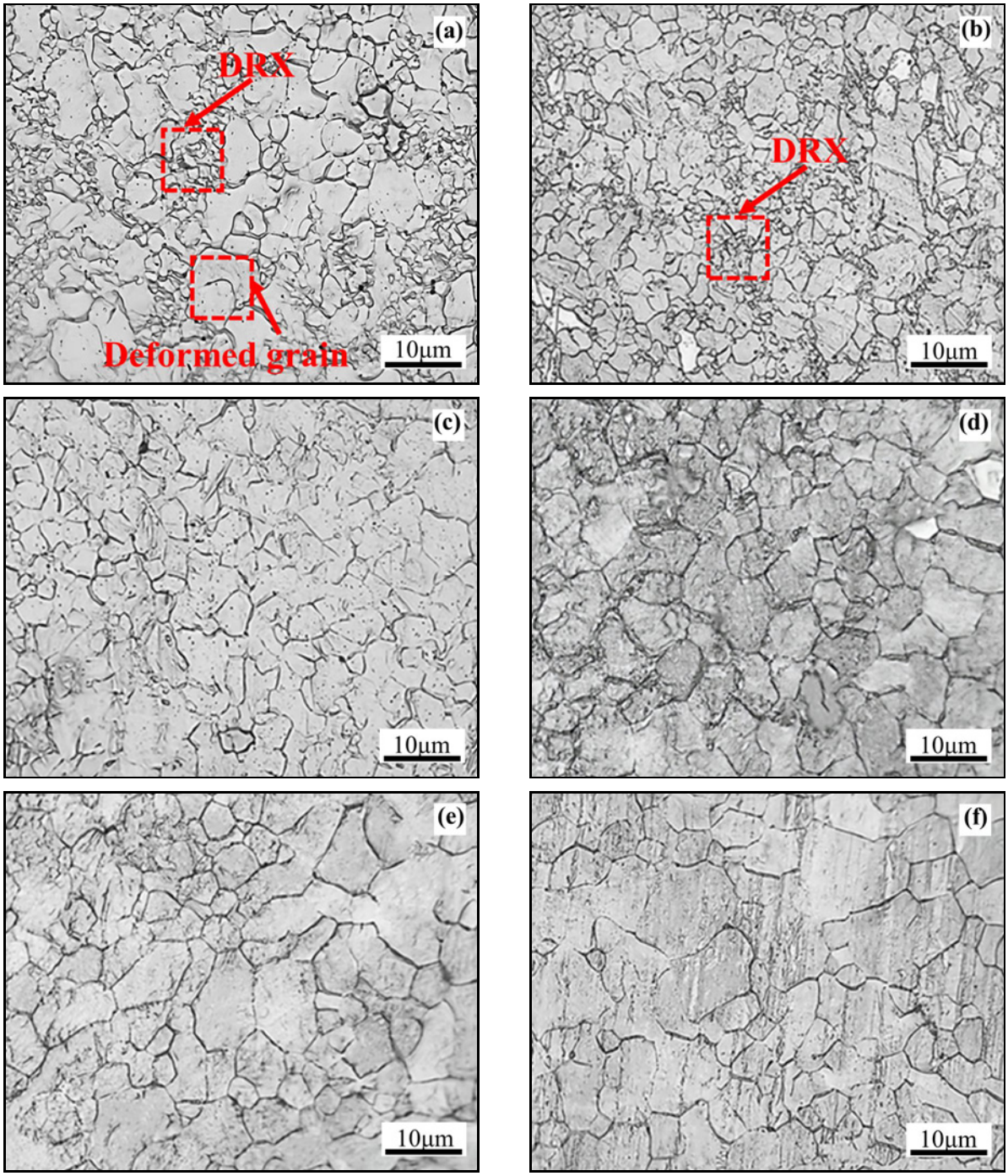

Fig. 2. Microstructure of Mg layer of Ti/Al/Mg/Al/Ti clad sheets under different annealing conditions: (a) as-rolled, (b) 200 °C/0.5 h, (c) 200 °C/1 h, (d) 200 °C/2 h, (e) 300 °C/2 h, and (f) 400 °C/2 h.

shown in Fig. 3, the Ti/Al bonding interface showed a straight line without obvious holes and defects, indicating that the Ti and Al layers were bonded well. The Al/Mg bonding interface showed an irregular wave shape because the 6061 and AZ31B have similar mechanical properties. Therefore, in the process of hot rolling, the Al layer and Mg layer in the clad sheets will undergo a large plastic deformation to achieve the metallurgical bond.

Figure 4 shows the EDS line scanning across Ti/Al and Mg/Al bonding interfaces of clad sheets obtained under different annealing conditions. With the increase of annealing time and annealing temperature, the thickness of the diffusion layer at the Ti/Al and the Mg/Al bonding interfaces continued to increase, and the thicknesses of the diffusion layers are shown in Table 5. The table shows that under the same annealing conditions, the thickness of the diffusion layer at

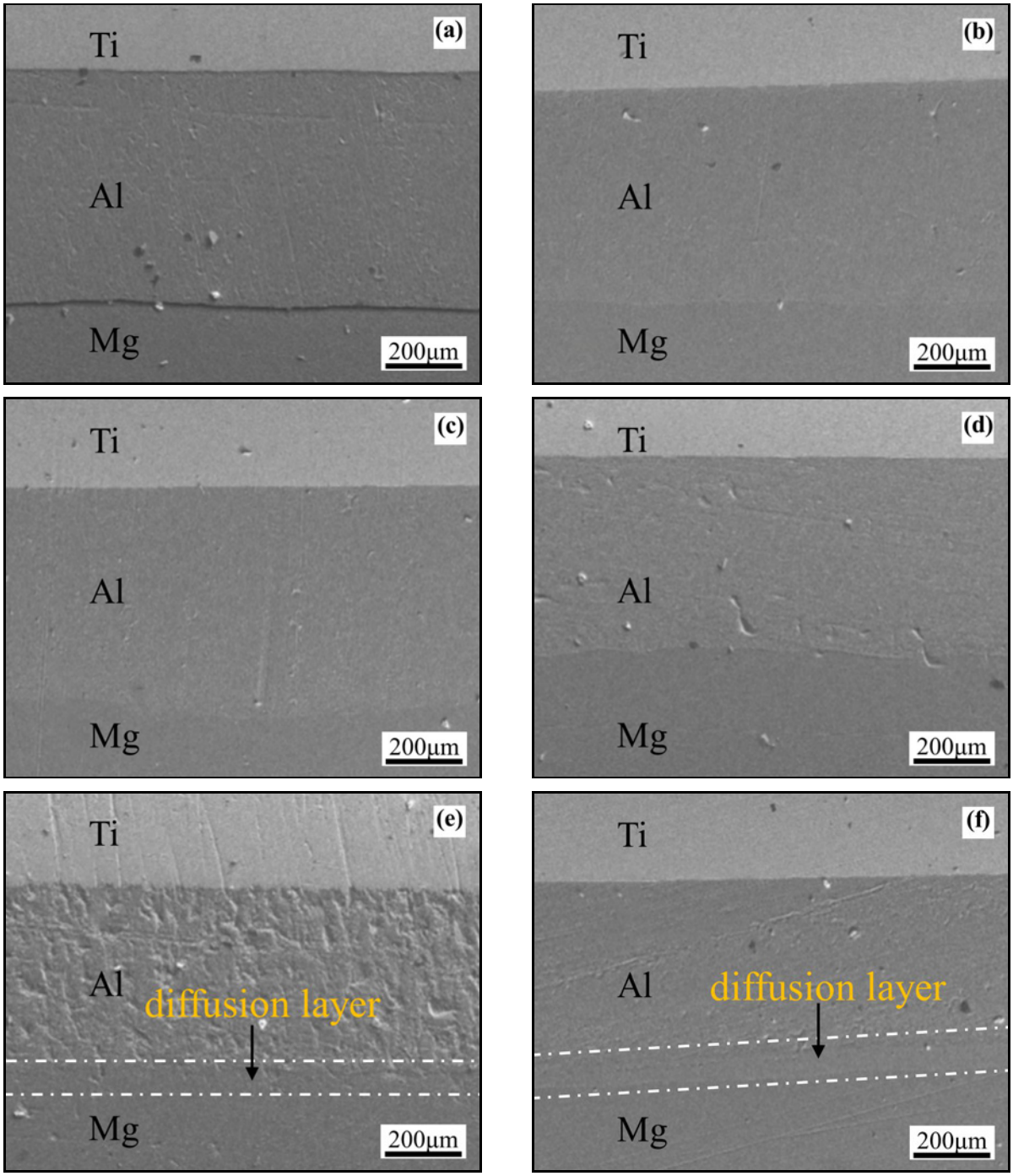

Fig. 3. Ti/Al/Mg/Al/Ti clad sheets bonding interface morphology and line scan element diffusion distribution of each layer: (a) as-rolled, (b) 200 ℃/0.5 h, (c) 200 ℃/1 h, (d) 200 ℃/2 h, (e) 300 ℃/2 h, and (f) 400 ℃/2 h.

the Ti/Al bonding interface was smaller than that at the Mg/Al bonding interface. In particular, the thickness of the diffusion layer at the Mg/Al interface increases substantially to 69.36 μm at 400 ℃, while the thickness of the diffusion layer at the Ti/Al interface at this temperature is only 4.61 μm. This is because diffusion of the Al atoms is more likely to occur in the Mg alloy than in the Ti alloy under the same annealing conditions. It can also be found that the effect of temperature on the diffusion rate of atoms is small at lower temperatures and increases when it exceeds a certain temperature. When the annealing temperature exceeded 300 ℃, the Mg/Al interface appeared as a continuous diffusion layer as in the white dashed box in Figs. 4e,f, and it can be found that the thickness of the diffusion layer at 400 ℃ was significantly larger than that at 300 ℃.

To further analyze the main compositions of the

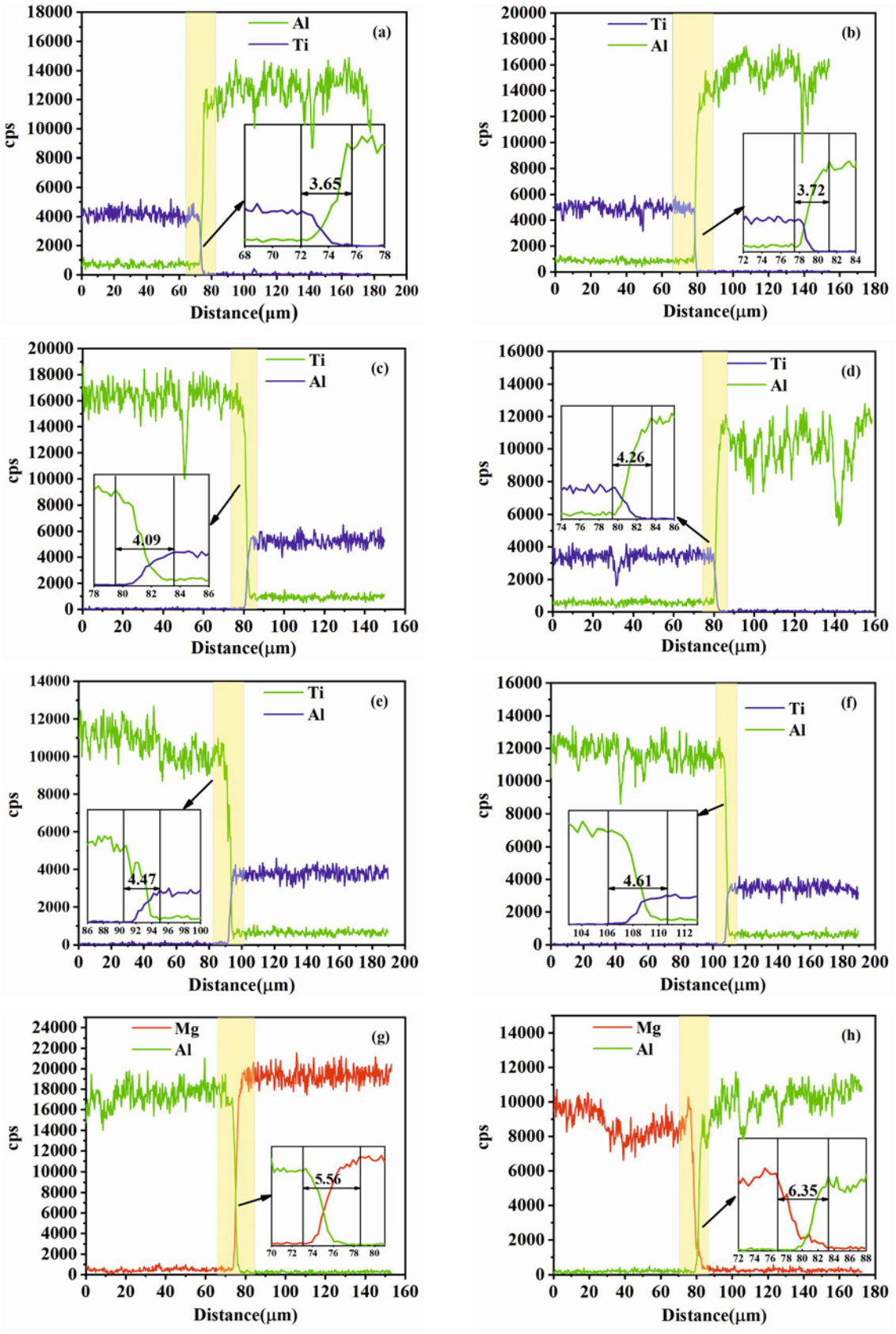

Fig. 4a–g. EDS line scanning across Ti/Al and Mg/Al interfaces of clad sheets obtained with different annealing conditions: (a) and (g) as-rolled, (b) and (h) 200 ℃/0.5 h, (c) and (i) 200 ℃/1 h, (d) and (j) 200 ℃/2 h, (e) and (k) 300 ℃/2 h, (f) and (l) 400 ℃/2 h.

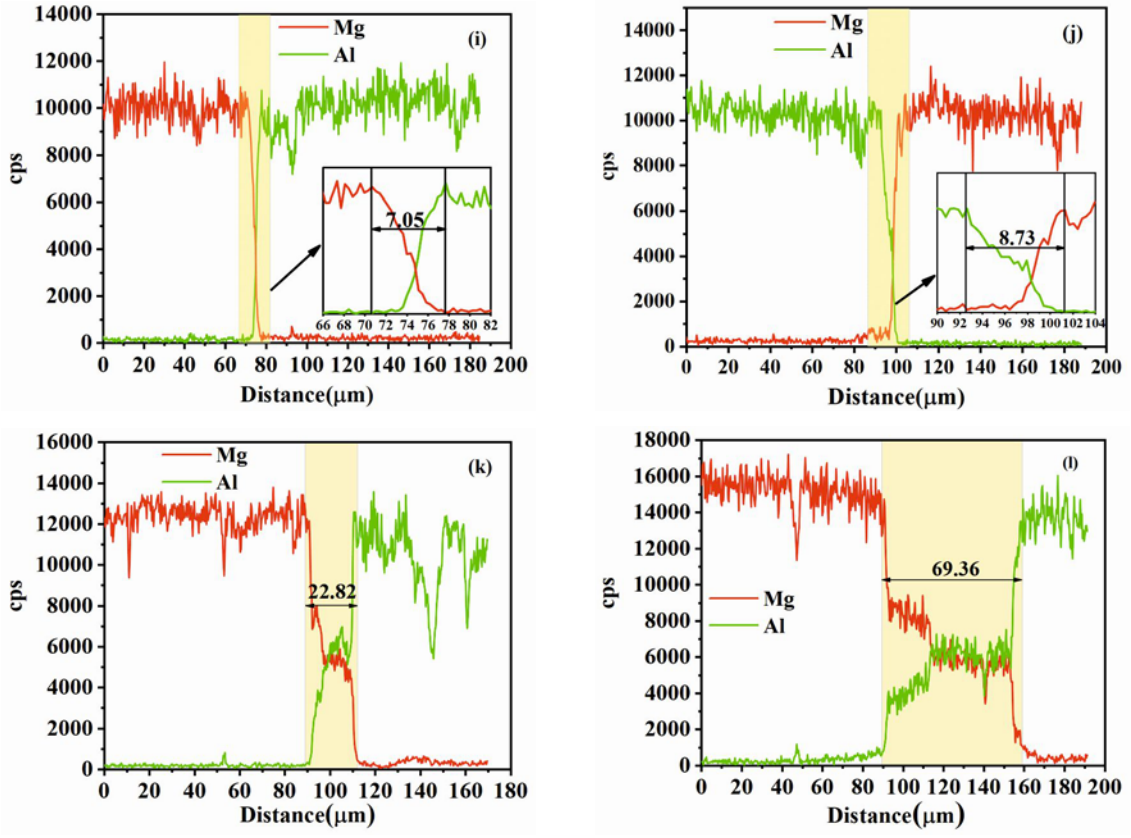

Fig. 4i–l. EDS line scanning across Ti/Al and Mg/Al interfaces of clad sheets obtained with different annealing conditions: (a) and (g) as-rolled, (b) and (h) 200 ℃/0.5 h, (c) and (i) 200 ℃/1 h, (d) and (j) 200 ℃/2 h, (e) and (k) 300 ℃/2 h, (f) and (l) 400 ℃/2 h.

Table 5. Thickness of the diffusion layer at the bonding interface under different annealing conditions

Annealing condition (℃ h^{-1})	Ti/Al interface (μm)	Mg/Al interface (μm)
As-rolled	3.65	5.56
200 ℃/0.5 h	3.72	6.35
200 ℃/1 h	4.09	7.05
200 ℃/2 h	4.26	8.73
300 ℃/2 h	4.47	22.8
400 ℃/2 h	4.61	69.36

intermediate compounds in the diffusion layer at the Mg/Al interface, the diffusion layer was subjected to EDS point scanning, as shown in Fig. 5. The specific gravities of Mg and Al atoms in the intermediate compound near the Mg layer were about 57.8 %, 42.2 % and 56.9 %, 43.0 %, respectively, so it was considered that the generated compound was $Mg_{17}Al_{12}$. The specific gravities of Mg and Al atoms in the intermediate compound near the Al layer side were about 39.2 %, 60.8 % and 41.0 %, 59.0 %, respectively, and it was considered that Al_3Mg_2 was generated. These two intermediate compounds, $Mg_{17}Al_{12}$ and Al_3Mg_2, are brittle compounds, and excessive intermediate compounds will seriously reduce the bonding strength of the clad sheets [26–28]. Therefore, the annealing system of the plate should be reasonably controlled to optimize the overall performance of clad sheets.

3.3. Hardness test

Figure 6 shows the hardness value of each layer region of the clad sheets under different annealing conditions. It can be seen from Fig. 6a that in the clad sheet in the rolled state, the hardness from the center of the Ti layer to the Al/Mg interface gradually decreased due to a small amount of Ti element diffused into the Al layer at the Ti/Al interface, so the hardness value of the Ti/Al interface was higher than

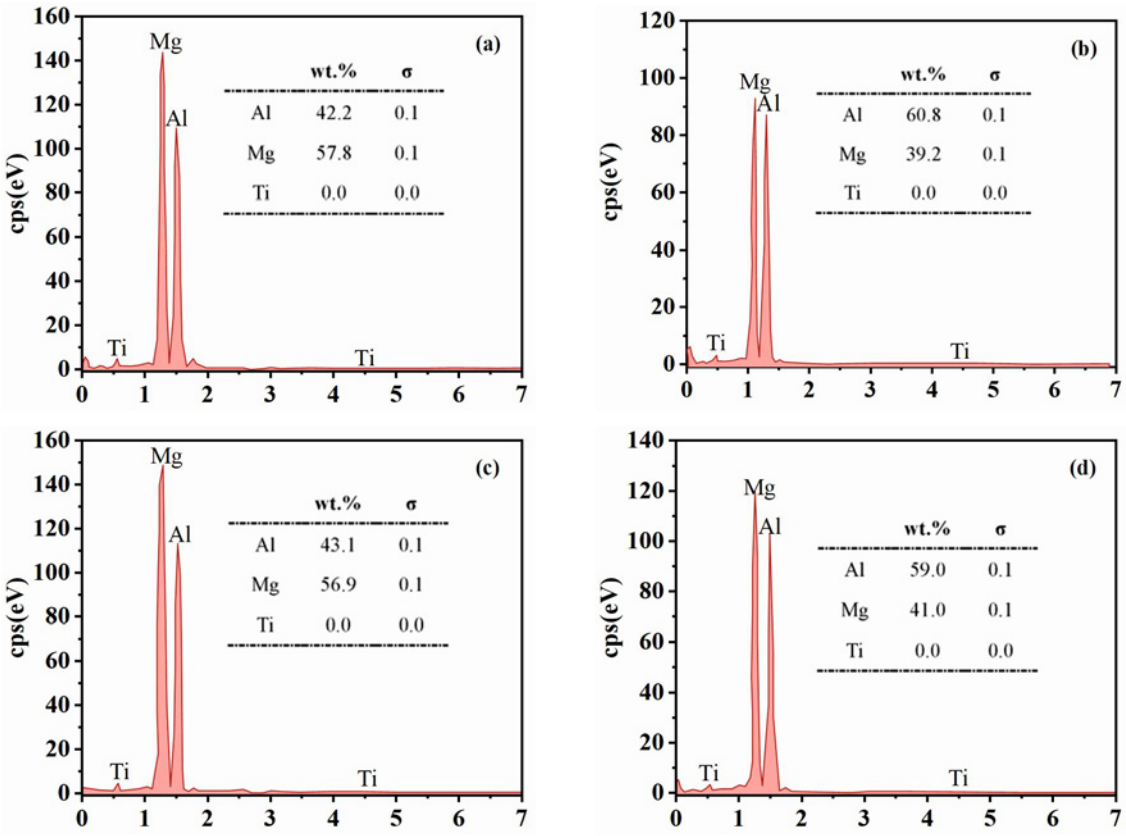

Fig. 5. Element distribution at the bonding interface: (a) and (b) Mg/Al interface point scanning at 300 ℃/2 h, (c) and (d) Mg/Al interface point scanning at 400 ℃/2 h.

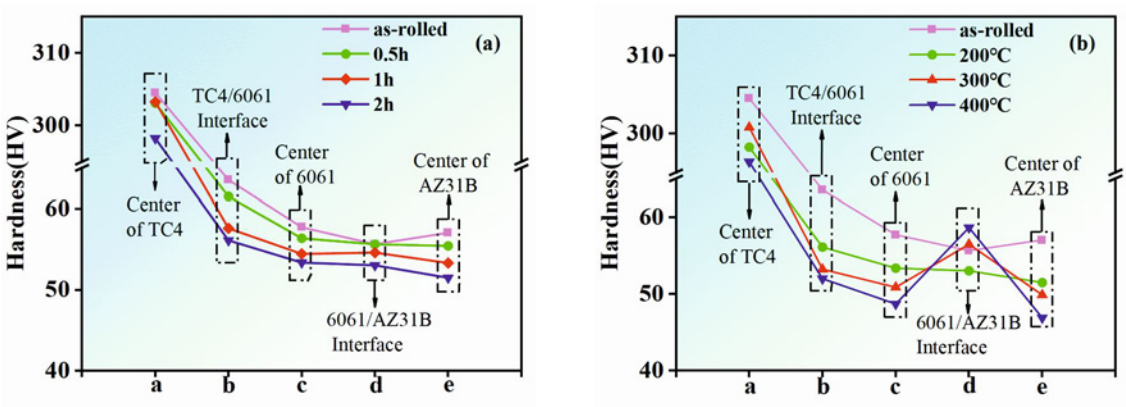

Fig. 6 Hardness values of each layer of Ti/Al/Mg/Al/Ti clad sheets: (a) under different annealing times and (b) under different annealing temperatures.

the center of the Al layer. The hardness value of the Mg layer center was slightly higher than the Al/Mg interface because during the rolling process, the dynamic recrystallization of the Mg layer made the Mg layer grains smaller, and the fine crystal strengthening effect was strengthened. However, after annealing, a large number of recrystallization occurred in the Mg layer, and the microstructure was gradually homogeneous, which made the hardness value of the Mg layer lower than the center of the Al layer.

In the annealed state, due to the recrystallization occurring in the Mg layer and Al layer, with the increase of the annealing time, the softening effect was strengthened. The hardness values of the Ti/Al/Mg/Al/Ti clad sheets were gradually reduced and lower than those in the rolled state. However, the element diffusion phenomenon occurred at the interface with increased annealing time, which differed from the rolled state. Part of the Al element diffused to the Mg layer to improve the hardness of the Mg

Table 6. YS, YTS, and EL of Ti/Al/Mg/Al/Ti clad sheets at different annealing time

Annealing time (h)	YS (MPa)	YTS (MPa)	EL (%)
0	462.82	485.53	19.58
0.5	465.51	495.76	20.07
1	453.06	486.42	21
2	483.72	511.5	22.03

layer, resulting in the hardness value of the Mg/Al interface being higher than the center of the Mg layer.

When the annealing time was 2 h, the variation of each hardness value of the Ti/Al/Mg/Al/Ti clad sheets with annealing temperature is shown in Fig. 6b. From Fig. 6b, it can be seen that with the increase of annealing temperature, the hardness value of each region of the clad sheets still showed a decreasing trend. This is because with the increase of the annealing temperature, the activity of the atoms in each layer was further improved, and the Al layer and Mg layer continued to recover and recrystallize so that the hardness value of each region was consistent with the trend when the annealing time increased. However, when the annealing temperatures were 300 and 400 ℃, the hardness value at the Al/Mg interface was higher than the hardness of the centers of the Al layer and Mg layer. The reason was that when the temperature exceeded 300 ℃, the Al/Mg interface generated two brittle compounds, Al_3Mg_2 and $Mg_{17}Al_{12}$, whose hardness was higher than the hardness of the Al layer and Mg layer.

3.4. Tensile properties test

When the annealing temperature was 200 ℃, the stress-engineering strain curves and the variation of the YS, the UTS, and the EL at different annealing times are shown in Fig. 7. It can be seen from Fig. 7 that the EL increased with the increase of annealing time, and the UTS increased slightly. The UTS decreased when the annealing time was 1 hour. Then, the YS and the UTS reached the maximum values of 483.72 and 511.5 MPa, respectively, when the annealing time was 2 h. According to the Hall-Page formula, the YS has a linear relationship with the inverse of the square root of the diameter of the grains in materials. Therefore, the more fine grains, the higher the grain boundary number, and the strengthening effect of the grain boundary was enhanced, which improved the strength of the clad sheets. However, when the annealing time was 0.5 or 1 h, dynamic recrystallization grains in rolling deformation and the recrystallization grains in the annealing process began to grow, and the number of grain boundaries decreased, so the UTS of clad sheets reduced. When the annealing time was 2 h, the recrystallization reached the maximum, the dislocation density of the Mg layer was reduced, and the storage energy generated in the rolling deformation was released to a great extent. At this time, the Mg layer microstructure was mainly dominated by fine and relatively uniform isoaxial grains, so the strength of the clad sheets was improved.

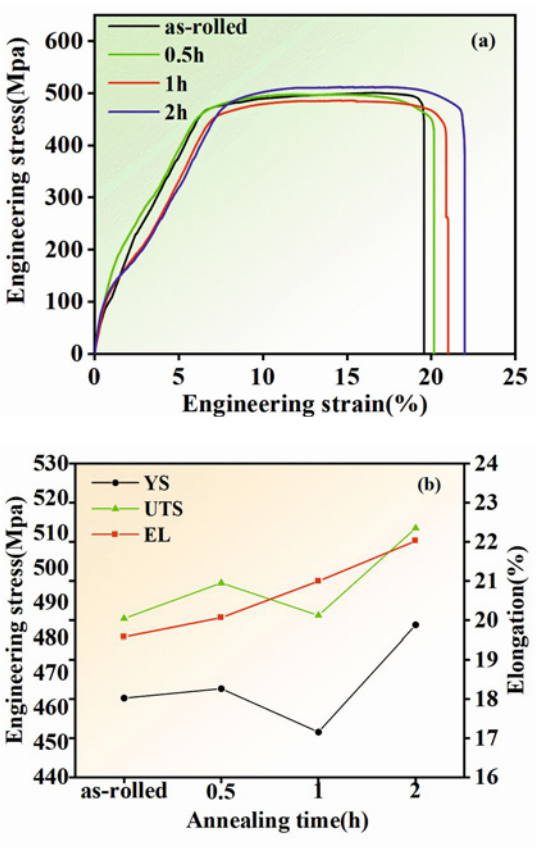

Fig. 7. Tensile properties of Ti/Al/Mg/Al/Ti clad sheets at different annealing times: (a) stress-strain curve and (b) mechanical properties.

When the annealing time was 2 h, the Mg layer microstructure was basically fine isoaxial grains, whose strain degree was not much different from that at the grain boundary so that the deformation was more uniform and the chance of cracking caused by stress concentration was greatly reduced. Therefore, the clad sheets can generate a large amount of deformation before fracture, the EL was improved to the maximum value of 21.48 %, which indicates that appropriate annealing of the rolled sheets can improve the plasticity of the clad sheets. Table 6 shows the values of the YS,

Table 7. YS, YTS, and EL of Ti/Al/Mg/Al/Ti clad sheets at different annealing temperatures

Annealing temperature (℃)	YS (MPa)	YTS (MPa)	EL (%)
0	462.82	501.53	19.58
200	483.72	511.50	22.03
300	425.98	457.56	12.64
400	435.66	473.00	10.92

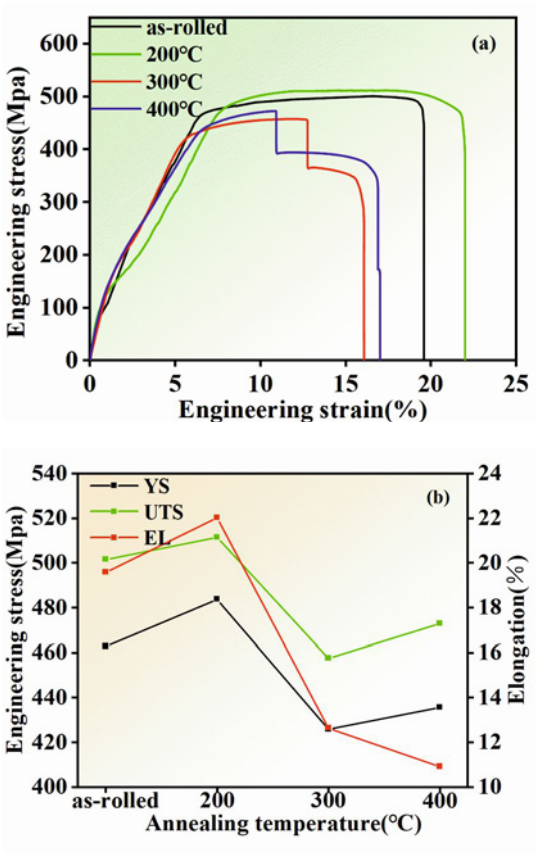

Fig. 8. Tensile properties of Ti/Al/Mg/Al/Ti clad sheets at different annealing temperatures: (a) stress-strain curve and (b) mechanical properties.

UTS, and EL of the clad sheets at different annealing times.

When the annealing time was 2 h, the stress-engineering strain curves and the variation of the YS, UTS, and EL at different annealing temperatures are shown in Fig. 8. From Fig. 8, it can be seen that when the annealing temperatures were 300 and 400 ℃, the stress drop occurred twice in the tensile curves. Figure 5 shows that two brittle compounds, Al_3Mg_2 and $Mg_{17}Al_{12}$, were generated at the Mg/Al interface. During the tensile process, the brittle compounds were separated first, which led to the fracture of the Mg layer, and the first stretch platform appeared. Then, the Al and Ti layers were subjected to the tensile force together until fracture occurred, and the second tensile platform appeared. The two stress drops caused a significant reduction in the EL, which reduced the plastic deformation capacity [29–31]. Table 7 shows the YS, UTS, and EL of the clad sheets at different annealing temperatures. From the table, it can be visualized the mechanical properties of the clad sheets are optimal at 200 ℃ for 2 h, and the YS, the UTS, and the EL reached maximum values of 483.72 MPa, 511.5 MPa, and 22.03 %.

3.5. Tensile fracture analysis

Figure 9 shows the tensile fracture morphology of the Ti/Al/Mg/Al/Ti clad sheets under different annealing conditions. From Figs. 9a–d, it can be seen that there were many dimples in the fracture of the Ti layer, and these dimples deepened gradually with the increase of the annealing time. Therefore, it is considered that the Ti layer was a ductile fracture in various annealing time periods. In the rolling state, there were many large and deep dimples in the fracture of the Al layer. When the annealing time was 0.5 h, the dimples in the fracture of the Al layer were very shallow. However, as the annealing time increased to 2 h, there were large and deep dimples on the fracture surface of the Al layer, which were surrounded by a dense circle of small and shallow dimples. Therefore, the Al layer also broke with ductile fracture at different annealing times. The dimples of the Mg layer fracture in the rolling state were shallow, and the number was small. When the annealing holding time was 0.5 h, the fracture morphology was familiar with the rolling state. When the annealing time was 1 h, the fracture dimples became deeper, and the number increased. When the annealing time was 2 h, the number of dimples increased significantly, and the dimples became deeper. Therefore, the Mg layer also fractured ductilely from the rolling state to the annealing at 200 ℃ for 2 h. Although the failure modes of each layer of the clad sheets under tensile load were ductile fracture at 200 ℃ annealing temperature, it can be seen that the plastic effect of each layer of the clad sheets was the best when the annealing holding time was 2 h, which was consistent with the results of tensile test.

From Figs. 9d–f, it can be seen that when the annealing temperature was 300 ℃, the fracture morphology of the Ti layer was similar to that at 200 ℃, and there were still many small dimples, which was a typi-

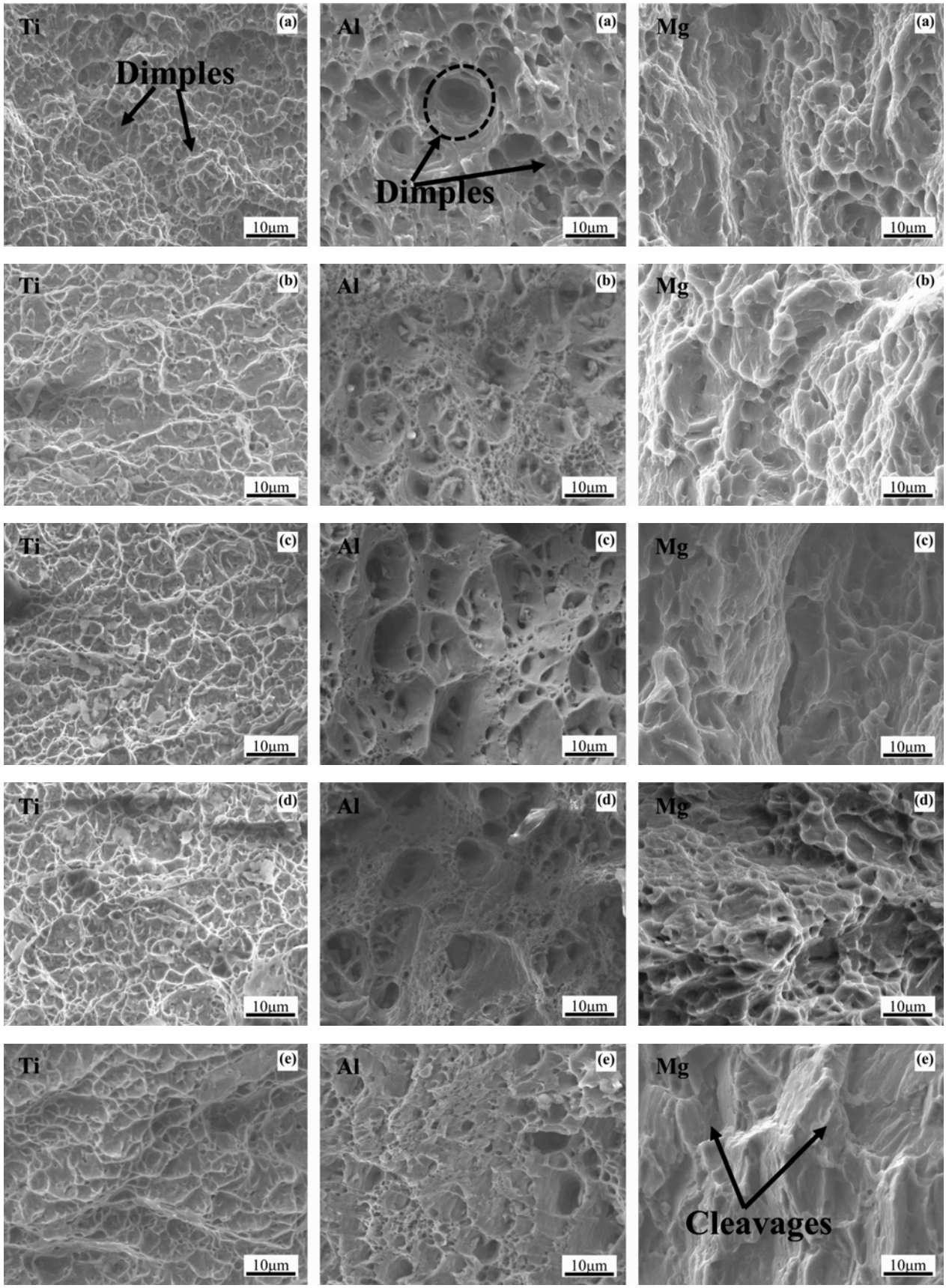

Fig. 9a–e. Fracture morphology of each layer in Ti/Al/Mg/Al/Ti clad sheets under different annealing conditions: (a) as-rolled, (b) 200 ℃/0.5 h, (c) 200 ℃/1 h, (d) 200 ℃/2 h, (e) 300 ℃/2 h.

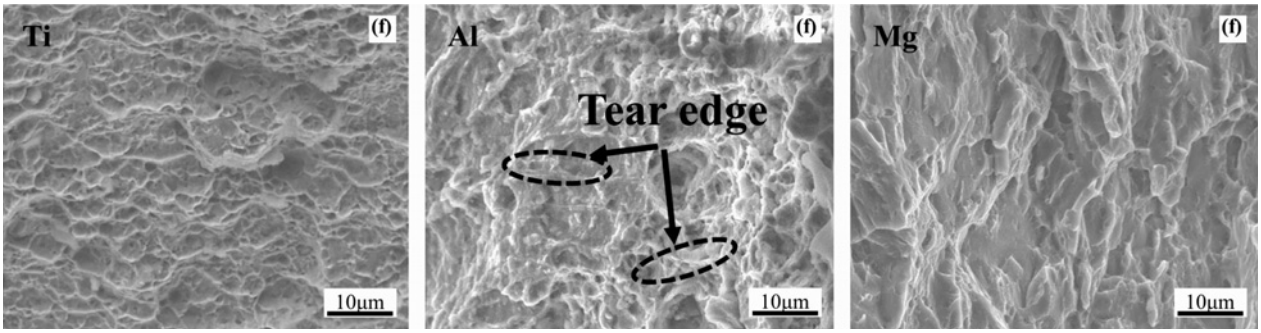

Fig. 9f. Fracture morphology of each layer in Ti/Al/Mg/Al/Ti clad sheets under different annealing conditions: (f) 400 ℃/2 h.

cal ductile fracture. When the annealing temperature was 400 ℃, the dimple size of the fracture of the Al layer became smaller and shallower than at 200 ℃, and there was an obvious tearing edge. The failure mode is a ductile fracture. It should be pointed out that the fracture of the Mg layer changed the most obviously with the increase in annealing temperature. Compared with the annealing temperature of 200 ℃, when the temperature rose to 300 ℃, the number of dimples in the fracture decreased greatly, and many cleavage planes and cleavage steps appeared. At this time, it was considered that the Mg layer had both ductile fracture and brittle fracture characteristics, which belonged to mixed fracture. When the annealing temperature increased to 400 ℃, the dimples in the fracture of the Ti layer became less and shallower but still belonged to ductile fracture. With the increase of annealing temperature, the size of dimples in the fracture of the Al layer became smaller, but there were still obvious tearing edges, which belonged to ductile fracture. The dimples in the fracture of the Mg layer at 400 ℃ disappeared. Compared with the 200 ℃ annealing temperature, the cleavage fracture of the river pattern appears in the magnesium layer, so it is considered that the mixed fracture of the Mg layer occurred under this annealing condition. By comparing the fracture morphology of the clad sheets under different annealing conditions, it can be concluded that the overall plasticity of the Ti/Al/Mg/Al/Ti clad sheets was the best under the annealing temperature of 200 ℃ for 2 h, which was consistent with the results obtained from the previous tensile test. The clad sheets under this condition had a maximum elongation of 21.48 %.

4. Conclusions

1. When the annealing time is 2 h, and the annealing temperature is 200 ℃, the grains in the Mg layer are equiaxed, and the grain size is uniform. When the annealing temperature exceeds 200 ℃, the grains of the magnesium layer will recrystallize and continue to grow.

2. When the annealing time is 2 h, and the annealing temperature reaches above 300 ℃, the hardness value of the Mg/Al interface is greater than that of the center of the aluminum layer and the center of the magnesium layer because of the generation of the intermediate compounds Al_3Mg_2 and $Mg_{17}Al_{12}$.

3. With the increase in annealing time and annealing temperature, the element diffusion layer thickness at the Ti/Al and Al/Mg interface increases.

4. When the annealing temperature is 200 ℃, the UTS of Ti/Al/Mg/Al/Ti clad sheets increases first, then decreases, and then increases again, but the UTS at each annealing time changes little. The elongation of the clad sheets will gradually increase with the increase of annealing time, reaching a maximum elongation of 21.48 % at 2 h annealing time.

5. When the annealing time is 2 h, the UTS of the clad sheets decreases with the increase of the annealing temperature, and when the annealing temperature reaches above 300 ℃, the secondary stress drop occurs during the tensile process. The elongation of the clad sheets will decrease significantly with the increase in annealing temperature.

6. Under different annealing times at 200 ℃, the ductile fracture occurs in each layer of the clad sheets. When the annealing temperature reaches above 300 ℃, the dimples of the aluminum layer decrease, and obvious tearing edges appear. At this time, the number of dimples in the fracture of the magnesium layer begins to decrease, and there are many dissociation steps. The failure mode of the magnesium layer is mixed fracture.

Acknowledgements

The authors are grateful for the financial support from the National Natural Science Foundation of China (No. 52375361) and the Major Science and Technology Project in Shanxi Province of China (No. 20181102015).

References

[1] J. M. Lanzon, M. J. Cardew-Hall, P. D. Hodgson, Characterising frictional behaviour in sheet metal forming, J. Mater. Process. Tech. 80–81 (1998) 251–256. https://doi.org/10.1016/S0924-0136(98)00110-1

[2] Z. P. Mao, J. P. Xie, A. Q. Wang, W. Y. Wang, D. Q. Ma, P. Liu, Effects of annealing temperature on the interfacial microstructure and bonding strength of Cu/Al clad sheets produced by twin-roll casting and rolling, J. Mater. Process. Tech. 285 (2020) 116804. https://doi.org/10.1016/j.jmatprotec.2020.116804

[3] T. Wang, Y. Y. Qi, J. L. Liu, J. C. Han, Z. K. Ren, Q. X. Huang, Research progress of metal laminates roll bonding process at home and abroad, Journal of Harbin Institute of Technology 52 (2020) 42. https://doi.org/10.11918/202003114

[4] Q. Zhou, R. Liu, Q. Zhou, C. Ran, K. S. Fan, J. Xie, P. W. Chen, Effect of microstructure on mechanical properties of titanium-steel explosive welding interface, Mater. Sci. Eng. A 830 (2022) 142260. https://doi.org/10.1016/j.msea.2021.142260

[5] A. Cohades, A. Çetin, A. Mortensen, Designing laminated metal composites for tensile ductility, Mater. Design B 66 (2015) 412–420. https://doi.org/10.1016/j.matdes.2014.08.061

[6] T. T. Zhang, W. X. Wang, W. Zhang, Y. Wei, X. Q. Cao, Z. F. Yan, J. Zhou, Microstructure evolution and mechanical properties of an AA6061/AZ31B alloy plate fabricated by explosive welding, J. Alloy Compd. 735 (2018) 1759–1768. https://doi.org/10.1016/j.jallcom.2017.11.285

[7] X. P. Zhang, S. Castagne, T. H. Yang, C. F. Gu, J. T. Wang, Entrance analysis of 7075 Al/Mg-Gd-Y-Zr/7075 Al laminated composite prepared by hot rolling and its mechanical properties, Mater. Design 32 (2011) 1152–1158. https://doi.org/10.1016/j.matdes.2010.10.030

[8] H. S. Liu, B. Zhang, G. P. Zhang, Microstructures and mechanical properties of Al/Mg alloy multilayered composites produced by accumulative roll bonding, J. Mater. Sci. Technol. 27 (2011) 15–21. https://doi.org/10.1016/S1005-0302(11)60019-4

[9] Z. Cheng, S. X. Wang, H. X. Qiao, Z. J. Chen, T. Q. Mo, Q. Liu, Enhancing the mechanical properties of hot roll bonded Al/Ti laminated metal composites (LMCs) by pre-rolling diffusion process, Metals 9 (2019) 795. https://doi.org/10.3390/met9070795

[10] X. Chen, G. S. Huang, S. S. Liu, T. Z. Han, B. Jiang, A. T. Tang, Y. Zhu, Grain refinement and mechanical properties of pure aluminum processed by accumulative extrusion bonding, T. Nonferr. Metal. Soc. 29 (2019) 437–447. https://doi.org/10.1016/S1003-6326(19)64953-8

[11] Y. C. Xin, R. Hong, B. Feng, H. H. Yu, Y. Wu, Q. Liu, Fabrication of Mg/Al multilayer plates using an accumulative extrusion bonding process, Mater. Sci. Eng. A 640 (2015) 210–216. https://doi.org/10.1016/j.msea.2015.06.008

[12] P. Chen, H. G. Huang, C. Ji, X. Zhang, Z. H. Sun, Bonding strength of Invar/Cu clad strips fabricated by twin-roll casting process, T. Nonferr. Metal. Soc. 28 (2018) 2460–2469. https://doi.org/10.1016/S1003-6326(18)64892-7

[13] H. G. Huang, Y. K. Dong, M. Yan, F. S. Du, Evolution of bonding interface in solid-liquid cast-rolling bonding of Cu/Al clad strip, T. Nonferr. Metal. Soc. 27 (2017) 1019–1025. https://doi.org/10.1016/S1003-6326(17)60119-5

[14] J. H. Zhang, S. J. Liu, R. Z. Wu, L. G. Hou, M. L. Zhang, Recent developments in high-strength Mg-RE-based alloys: Focusing on Mg-Gd and Mg-Y systems, J. Magnes. Alloy 6 (2018) 277–291. https://doi.org/10.1016/j.jma.2018.08.001

[15] T. Tokunaga, M. Ohno, K. Matsuura, Coatings on Mg alloys and their mechanical properties: A review, J. Mater. Sci. Technol. 34 (2018) 1119–1126. https://doi.org/10.1016/j.jmst.2017.12.004

[16] Z. Q. Chen, D. Y. Wang, X. Q. Cao, W. W. Yang, W. X. Wang, Influence of multi-pass rolling and subsequent annealing on the interface microstructure and mechanical properties of the explosive welding Mg/Al composite plates, Mater. Sci. Eng. A 723 (2018) 97–108. https://doi.org/10.1016/j.msea.2018.03.042

[17] H. H. Nie, W. Liang, H. S. Chen, L. W. Zheng, C. Z. Chi, X. R. Li, Effect of annealing on the microstructures and mechanical properties of Al/Mg/Al laminates, Mater. Sci. Eng. A 732 (2018) 6–13. https://doi.org/10.1016/j.msea.2018.06.065

[18] X. P. Zhang, T. H. Yang, S. Castagne, J. T. Wang, Microstructure, bonding strength and thickness ratio of Al/Mg/Al alloy laminated composites prepared by hot rolling, Mater. Sci. Eng. A 528 (2011) 1954–1960. https://doi.org/10.1016/j.msea.2010.10.105

[19] J. J. Zhang, W. Liang, H. T. Li, Effect of thickness of interfacial intermetallic compound layers on the interfacial bond strength and the uniaxial tensile behaviour of 5052 Al/AZ31B Mg/5052 Al clad sheets, RSC Adv. 5104954–104959. https://doi.org:10.1039/C5RA15357C

[20] P. J. Wang, Z. J. Chen, C. Hu, B. X. Li, T. Q. Mo, Q. Liu, Effects of annealing on the interfacial structures and mechanical properties of hot roll bonded Al/Mg clad sheets, Mater. Sci. Eng. A 792 (2020) 139673. https://doi.org/10.1016/j.msea.2020.139673

[21] A. X. Zhang, F. Li, P. D. Hua, W. T. Niu, R. H. Gao, Response mechanism of matrix microstructure evolution and mechanical behavior to Mg/Al composite plate by hard-plate accumulative roll bonding, J. Mater. Res. Technol. 23 (2023) 3312–3321. https://doi.org/10.1016/j.jmrt.2023.01.227

[22] Y. J. Mi, H. H. Nie, T. L. Wang, X. R. Li, X. W. Hao, W. Liang, Effect of anisotropy on microstructures and mechanical properties of rolled Ti/Al/Mg/Al/Ti laminates, J. Mater. Eng. Perform. 28 (2019) 4143–4151. https://doi.org/10.1007/s11665-019-04172-2

[23] T. L. Wang, H. H. Nie, Y. J. Mi, X. W. Hao, F. Yang, C. Z. Chi, W. Liang, Microstructures and mechanical properties of Ti/Al/Mg/Al/Ti laminates with various rolling reductions, J. Mater. Res. 34 (2019) 344–353. https://doi:10.1557/jmr.2018.428

[24] P. J. Wang, Z. J. Chen, H. T. Huang, J. S. Lin, B. X. Li, Q. Liu, Fabrication of Ti/Al/Mg laminated composites by hot roll bonding and their microstructures and mechanical properties, Chinese J. Aeronaut. 34 (2021) 192–201. https://doi.org/10.1016/j.cja.2020.08.044

[25] H. H. Nie, L. W. Zheng, X. P. Kang, X. W. Hao, X. R. Li, W. Liang, In-situ investigation of deformation

behavior and fracture forms of Ti/Al/Mg/Al/Ti laminates, T. Nonferr. Metal. Soc. 31 (2021) 1656–1664. https://doi.org/10.1016/S1003-6326(21)65605-4

[26] T. T. Liu, B. Song, G. S. Huang, X. Q. Jiang, S. F. Guo, K. H. Zheng, F. S. Pan, Preparation, structure and properties of Mg/Al laminated metal composites fabricated by roll-bonding: A review, J. Magnes. Alloy 10 (2022) 2062–2093. https://doi.org/10.1016/j.jma.2022.08.001

[27] K. S. Lee, H. K. Kim, Y. M. Jo, S. E. Lee, J. Heo, Y. W. Chang, Y. S. Lee, Interface-correlated deformation behavior of a stainless steel-Al-Mg 3-ply composite, Mater. Charact. 75 (2021) 138–149. https://doi.org/10.1016/j.matchar.2012.10.012

[28] K. S. Lee, D. H. Yoon, H. K. Kim, Y. N. Kwon, Y. S. Lee, Effect of annealing on the interface microstructure and mechanical properties of a STS-Al-Mg 3-ply clad sheet, Mater. Sci. Eng. A 556 (2012) 319–330. https://doi.org/10.1016/j.msea.2012.06.094

[29] Y. P. Ren, N. H. Tariq, H. H. Liu, X. Y. Cui, J. Q. Wang, T. Y. Xiong, Unraveling the effects of hot rolling on microstructure and mechanical properties of cold sprayed Mg/Al clad plates, Mater. Today Commun. 33 (2022) 104553. https://doi.org/10.1016/j.mtcomm.2022.104553

[30] T. Wang, Z. F. Tang, L. Yang, L. Wu, H. Y. Yan, C. Liu, Y. Z. Ma, W. S. Liu, A novel technique for preparing Al/Mg alloy by the combined method of powder metallurgy and rolling, Mater. Lett. 314 (2022) 131793. https://doi.org/10.1016/j.matlet.2022.131793

[31] T. Wang, Y. L. Wang, L. P. Bian, Q. X. Huang, Microstructural evolution and mechanical behavior of Mg/Al laminated composite sheet by novel corrugated rolling and flat rolling, Mater. Sci. Eng. A 765 (2019) 138318. https://doi.org/10.1016/j.msea.2019.138318